Cross section data for the D(^{3}He,p)^{4}He nuclear reaction from 0.25 to 6 MeV

B. Wielunska, M. Mayer, T. Schwarz-Selinger, U. von Toussaint, J. Bauer

Max-Planck-Institut für Plasmaphysik, Boltzmannstr.2, 85748 Garching, Germany

Abstract

The differential cross sections for the nuclear reaction D(^{3}He, p)^{4}He were determined at reaction angles of 135°, 144.5° and 175° for ^{3}He energies in the laboratory frame between 0.25 and 5.6 MeV. The uncertainty of the determined cross sections is between 4.1% and 5.9%. The results were compared with theoretical predictions for the cross sections [M. Nocente et al., Nuclear Fusion 50 (2010) 055001]. For energies below 1 MeV the theoretical values deviate significantly from the experimental data. For higher energies the theoretical predictions agree well with the experimental data.

Introduction

The nuclear reaction D(^{3}He,p)^{4}He is commonly used to determine the depth profile of deuterium in solids [1, 2]. By analyzing the energy spectrum of the α-particles the depth profile in the near surface layer can be derived [3]. With the proton energy spectra the depth profile up to very large depths can be reconstructed: Up to depths of about 40 µm in low-Z materials and up to about 8 µm in heavy materials such as tungsten [2].

For nuclear reaction analysis (NRA) the differential cross section at a specific reaction angle is needed. The total cross section of this reaction has a broad resonance region around 630 keV and a non-resonant region at higher energies [1, 2]. Depth profiling to large depths requires the simultaneous fit of multiple measurements at different incident energies [2, 4], which requires precise cross section data over a large range of energies. Unfortunately most of the existing data in literature are limited to maximum ^{3}He energy of 2.5 MeV. Möller and Besenbacher measured very precisely the total cross section for this reaction by comparison to the D(d,p)T reaction, achieving an accuracy for the total cross section of 4% for energies from 0.2 MeV to 1.25 MeV and an accuracy of 5 % for energies up to 2.5 MeV [5]. Bosch and Hale used an energy dependent formula and the Padé polynomial expansion to represent the total cross sections resulting from R-matrix calculations from 1979. The Bosch/Hale fit to the total

cross section is valid in the lab energy range 0.75 to 12000 keV [6]. Nocente derived formulas based on Bosch and Hale and several fits to data for the angular dependence, thus allowing deriving the differential cross section at any angle [7]. To check this theoretical prediction and to obtain precise experimental differential cross section data, these were measured in the energy range from 0.25 MeV to 6 MeV at laboratory angles of 135°, 144.5°, and 175°.

Experimental

For determining the cross section, energy spectra of the protons from the D(^{3}He,p)4He nuclear reaction were recorded for different energies from 0.25 MeV to 6 MeV at reaction angles of 135°, 144.5°, 175°. As deuterium-containing target a dense, plasma- deposited amorphous deuterated thin hydrocarbon (a-C:D) film was grown on single crystalline silicon (100) substrates. The thickness of the film was measured with tactile profilometry to be 50 nm. The D/(C+D) ratio was assumed to be about 0.34 —consistent with a-C:H films deposited under the same conditions [8]. A 8.5 nm thick Au film was evaporated on the a-C:D film to make a dose correction of ^{3}He ions via RBS. All measurements were performed on one sample. The thickness of the Au film was determined by RBS at three points of the sample. The thickness homogeneity of the Au film was better than 99.5%. The ^{3}He beam was produced by the 3 MV tandem accelerator at the Max-Planck-Institut für Plasmaphysik in Garching. The accelerator terminal voltage was calibrated with the ^{27}Al(p,γ)^{28}Si resonances at 992 and 1380 keV. The beam energy spread is below 0.1% for protons at 1000 keV and it can be assumed that the spread is of the same order for higher energies. For ^{4}He ions the accelerator terminal voltage was calibrated with the ^{16}O(α,α)^{16}O resonances at 3036 and 3877 keV and is correct within 0.4–0.5%. The same accuracy is expected for 3He. The angle between the incident beam and the sample normal was 0°.The beam spot area is 1 mm^{2}.

The cross section was measured at three laboratory reaction angles. The detector located at an angle of 135° has a parabolic slit with a width of 3 mm and height of 17 mm. The detector target distance is about 40 mm. The solid angle is 29.18 msr. The detector's depletion depth is 2000 µm. The 144.5° detector aperture is circular with a diameter of 18 mm. The detector-target distance is 100 mm. The geometrical solid angle of this detector is 21.3 msr. The detector's depletion depth is 1500 µm thick. The detector at 175° is an annular detector with an inner diameter of 11.8 mm and an outer diameter of 17 mm. The detector - target distance is 84 mm. Its geometrical solid angle is 16.3 msr and it has a depletion depth of 2000 µm. In front of each

detector Nickel, Mylar absorber foils are installed to stop the backscattered ^{3}He ions. The foils in front of the 135° detector and the 144.5° detector consist of a 12 µm thick Mylar layer coated with 10 nm Gold and a 5 µm thick Nickel layer. In front of the annular detector at 175° a foil with 50 µm thick Mylar layer and 50 nm Au film is positioned. Only high-energetic protons created in nuclear reactions can penetrate the absorber foils. For our samples the high energetic protons from D(^{3}He,p)α, from the ^{12}C(^{3}He,p)^{14}N, from the ^{13}C(^{3}He, $p_{0,1,2}$)^{15}N and from the ^{28}Si(^{3}He, $p_{0,1,2,3,4}$)^{30}P reactions reach the detector. Protons from the ^{13}C(^{3}He,p)^{15}N reaction can overlap with protons from the D(^{3}He,p)α reaction at some incident energies [1]. However, as was already shown in [1], the amount of these protons is insignificant for our type of samples. In Fig. 1-3 one can see three typical proton energy spectra with the signal peak around 12 MeV. In Fig. 1 the spectrum at incident energy of 1000 keV is shown. Only protons from D(^{3}He,p)α reach the detector at this energy. For energies higher than 1.6 MeV we clearly see beside the signal peak also proton peaks from the nuclear reaction of ^{12}C(^{3}He,p)^{14}N, see Fig. 2 for incident energy 2.0 MeV. Protons from the ^{28}Si(^{3}He, $p_{0,1,2,3,4}$)^{30}P reaction begin to appear in the spectra at energies above 3 MeV see Fig. 3 for an incident energy of 4 MeV. At energies above 5.6 MeV these protons start to overlap with the signal from the D(^{3}He,p)α reaction: At these energies measurements with a silicon substrate start to become impossible.
The cross sections at 135° and 175° were measured simultaneously in the same setup. The cross section at 144.5° was measured in a different setup. An analyzing dose of 5 µC was collected for each data point. To minimize the influence of deuterium depletion due to ion-bombardment induced desorption, different spots on the target were used at each energy.
For each proton spectrum the background was determined and substracted.

Coincidentally to all NRA measurements backscattered ^{3}He ions were detected by a detector at a scattering angle of 165° with a solid angle of 1.1 msr. The cross section for backscattering of ^{3}He from Au is Rutherford at all used energies [9]. The backscattering signal from the Au layer was used to minimize possible errors of the beam current measurement. The beam current was measured using a negatively biased Faraday shield.

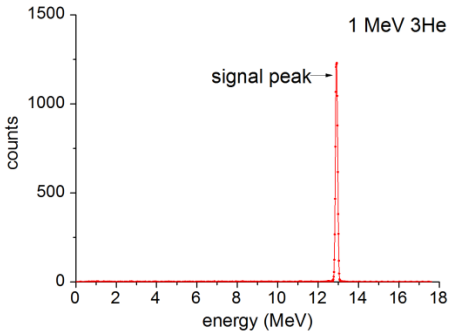

Fig.1: Proton energy spectrum at an ^{3}He incident energy of 1000 keV with the proton signal peak around 13 MeV in the 135° proton detector. The energy spectra from the other detectors look qualitatively similar.

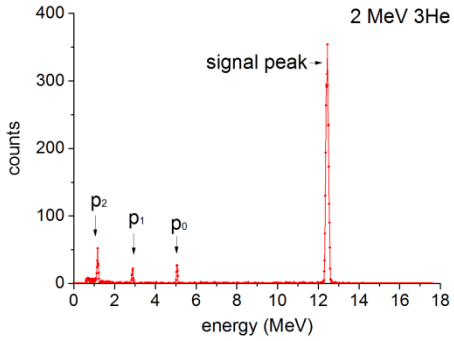

Fig. 2:Proton energy spectrum at ^{3}He incident energy of 2 MeV with the proton signal peak around 12.5 MeV from the 135° proton detector. The three proton peaks on the left are protons from the nuclear reaction $^{12}C(^{3}He,p)^{14}N$.

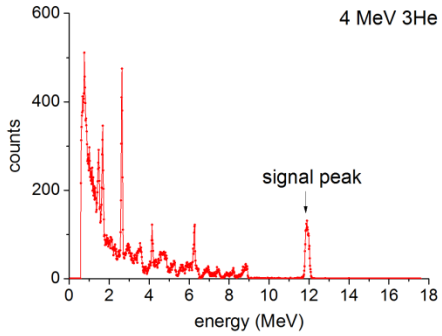

Fig. 3:Proton energy spectrum at ^{3}He incident energy of 4 MeV with the proton signal peak around 12 MeV from the 135° proton detector. Additional background from the nuclear reaction $^{28}Si(^{3}He,p_x)^{30}P$ appears in the spectrum. Proton peaks from $^{12}C(^{3}He,p)^{14}N$ are also visible.

To derive the cross section from the energy spectra the fact that the number of detected protons is proportional to the cross section was used. For every spectrum the numbers of counts of the proton signal peaks were determined. Plotting the count integrals versus the mean energy in the a-C:D layer gives the relative shape of the differential cross section. To get the mean energy in

the a-C:D layer the thicknesses of the gold layer and a:C-D layer are needed. The thickness of the gold layer is known from the RBS spectra. With the knowledge of the cross section at 135° and the D/(D+C) ratio of the a-C:D film the thickness of the a-C:D layer was determined from the proton peak at 135°. To obtain the mean energy the energy loss in the gold film and half of the energy loss in the a:C-D layer was subtracted from the incident energy. The energy loss is between 6.5 keV for the highest incident energy and 17.1 keV for the lowest energy. With this the relative shape of the differential cross section for the three angles was measured. The statistical uncertainties of the individual measurement points are the square roots of the count integrals of the signal peak, the background counts and the Au signal peak (Poisson distributions). The total uncertainty is the quadratic sum of these uncertainties as they are statistically independent. The uncertainties at 135° are between 0.8% and 4.2%. The uncertainty range at 144.5° is between 0.7% and 2.7% and at the 175° angle we get uncertainties between 1.3% and 4.3%.

To convert the relative measurements into absolute values in milibarn/steradiant the total cross section in the center of mass system from Möller and Besenbacher was used. The Möller Besenbacher cross section has an unsurpassed absolute accuracy of 4 % [5]. As the differential cross section in the center of mass system is angle independent for energies below 0.6 MeV and its angle dependence is smaller than 4% between 0° and 90° for energies up to 1700 keV [10] the differential cross section was derived for low energies (<1.2 MeV) [1] for any angle just by dividing the total cross section of Möller, Besenbacher by 4π in the center-of-mass system. In the next step this differential cross section was converted to the laboratory frame for the three desired reaction angles. As having now the differential cross section in the lab system for energies lower than 1.2 MeV the experimental data were fitted with a least square fit in the low energy range from 0.5 MeV to 1.2 MeV and the absolute values for our experimental data were obtained. As the influence of the energy loss of the incoming ^{3}He in the a-C:D layer is more than 4 % for low energies we restricted the fit between 0.5 and 1.2 MeV. The results for the 135°, 144.5° and 175° reaction angles are shown in Fig. 4- 6. Fig. 4 shows besides the measured data already published experimental data [1]. One can see that they agree within their error bars. This verifies the measured data at 135° and 175° as the measurements were done coincidentally. To obtain the total error of the individual points the 4 % uncertainty resulting from the accuracy of Möller/ Besenbacher has to be added quadratically to the errors described above. Table1 gives the results for the differential cross sections with the total errors in percent.

Energy (keV)	Differential cross section 135°	Total uncertainty in percent	Differential cross section 175°	Total uncertainty in percent	Energy (keV)	Differential cross section 144.5°	Total uncertainty in percent
232.9	7.5	4.6	7.5	5.3	184.2	3.6	4.8
282.0	13.1	4.4	13.0	4.8	282.0	13.4	4.2
331.3	20.4	4.2	21.9	4.5	380.9	30.7	4.1
380.9	30.3	4.2	31.5	4.3	480.6	48.0	4.1
430.6	39.1	4.1	40.4	4.3	530.6	56.5	4.1
480.6	48.6	4.1	50.2	4.2	610.8	60.4	4.1
530.6	54.7	4.1	55.4	4.2	671.0	56.1	4.1
580.7	59.2	4.1	57.7	4.2	781.6	50.1	4.1
610.8	59.4	4.1	57.3	4.2	882.2	43.4	4.1
630.8	59.3	4.1	54.5	4.2	982.8	35.1	4.1
681.1	60.3	4.1	55.1	4.2	1183.9	26.2	4.1
781.6	51.1	4.1	45.8	4.2	1385.0	20.3	4.2
982.8	36.7	4.1	33.7	4.3	1585.9	17.5	4.2
1183.9	26.6	4.2	27.0	4.4	1786.7	13.7	4.2
1385.0	21.4	4.3	19.5	4.6	1987.4	12.7	4.3
1585.9	17.1	4.3	15.6	4.7	2188.0	10.7	4.3
1786.7	14.6	4.4	13.8	4.8	2388.5	9.5	4.3
1987.4	12.2	4.5	10.7	5.0	2589.0	8.7	4.4
2188.0	11.3	4.5	9.5	5.1	2789.4	8.6	4.4
2388.5	10.1	4.6	8.6	5.2	2989.8	7.4	4.4
2589.0	9.1	4.6	8.1	5.3	3190.2	6.9	4.4
2789.4	8.1	4.7	7.7	5.4	3390.5	7.1	4.4
2989.8	7.7	4.8	8.0	5.4	3590.8	6.6	4.5
3190.2	7.5	4.8	6.6	5.6	3791.1	6.4	4.5
3390.5	7.0	4.9	6.7	5.6	3991.4	6.6	4.5
3590.8	7.0	4.9	6.9	5.6	4191.6	5.9	4.5
3791.1	6.7	4.9	6.9	5.6	4391.8	6.5	4.5
3991.4	6.4	5.0	6.8	5.7	4592.0	5.9	4.5
4391.8	6.0	5.1	6.8	5.7	4792.2	6.0	4.5
4792.2	6.5	5.2	7.6	5.7	4992.4		
5192.6	5.6	5.3	7.1	5.8	--		
5592.9	5.8	5.4	7.9	5.9	--		
5993.2	5.6	5.6	--	--	--		
6393.5	5.5	5.8	--	--	--		

Table1: experimental data at the reaction angle 135°,144.5°,175°

To get from these data points a smoothed curve for the cross section for all energies that can be used by simulating programs like SIMNRA, the data points were fitted by the equation (1) from [11]. The fit parameters for each detector are listed in Table 2.

$$y = A_0 \left(\frac{x^{A_1}(A_2 \exp(A_3 x) + A_4)}{x^{A_5} + A_2 \exp(A_6 x) + A_7} \right) \quad (1)$$

With x the energy in MeV.

Fit parameters	135°	144.5°	175°
A_0	48.7936	46.6387	51.1371
A_1	2.26056	2.30509	2.39582
A_2	1.24289	1.20427	1.26905
A_3	-1.39591	-1.29964	-1.51308
A_4	0.215408	0.196564	0.0466659
A_5	2.62926	2.60551	1.73512
A_6	-0.976554	-0.953374	-1.50454
A_7	-0.758929	-0.762614	-0.779459

Table2: Fit parameters for the three angles.

Comparison of data with theoretical predictions for differential cross section

Nocente provides a formula for the differential cross section of the D(^{3}He,p)α reaction based on fits to several data sets and the total cross section parametrizations from Bosch and Hale [6, 7].

The differential cross section $\frac{d\sigma}{d\Omega}$ is described depending on the energy in the center of mass (cm) system and on the cm scattering angle of the proton as:

$$\frac{d\sigma}{d\Omega}(\theta_p, E) = \frac{d\sigma}{d\Omega}(\theta_p = 0, E) \cdot \sum_{l=0}^{6} \sum_{k=0}^{5} \alpha_{lk} E^k P_l(cos(\theta_p)) \quad (2)$$

With

$$\frac{d\sigma}{d\Omega}(\theta_p = 0, E) = \frac{1}{4\pi \cdot \sum_{k=0}^{5} \alpha_{0,k} E^k} \cdot \sigma(E) \quad (3)$$

θ_p: reaction angle of the proton in the center of mass system

E: energy in the center of mass system

P_l: Legendre polynomials

α_{lk}: coefficients describing the energy dependence of the Legendre coefficients, obtained by fitting to data see [7]

$\sigma(E)$: total cross section

A detailed discussion of this formula and the values of the parameters $\alpha_{l,k}$, a_0 can be found in [7].

σ(E) is the total cross section for which the Bosch/Hale's parametrization is used [6]. The parametrization consists of an energy dependent form with a S-function (eq.(4)). The parametrization formula is:

$$\sigma(E) = \frac{S(E)}{E \cdot \exp\left(B_G / \sqrt{E}\right)} \tag{4}$$

E: energy in the center of mass system

B_G: Gamov constant

S: S-function

The S-function is described by Padé polynomials (eq. (5)).

$$S(E) = \frac{A1 + E\left(A2 + E\left(A3 + E(A4 + EA5)\right)\right)}{1 + E\left(B1 + E\left(B2 + E(B3 + EB4)\right)\right)} \tag{5}$$

This parametrization fits the total cross section which results from R- matrix calculations from 1979. For detailed information and values for the constants see [6].

Bosch and Hale give two parameter sets for A1-A6 and B1-B4 depending on the cm energy. There is one parameter set for cm energies from 0.3 keV to 900 keV which corresponds to 0.75 keV – 2250 keV for the ^{3}He incident energy in the laboratory frame. The other parameter set is for cm energies up to 4800 keV which corresponds to 12000 keV in the lab frame. With this formulas and parametrizations of the two publications the differential cross sections for the D(^{3}He,p)α reaction at laboratory energies between 0 keV and 6000 keV for 135°, 144.5°, 175° reaction angles were calculated. These theoretical results are compared to the measured data points in Figs. 4 – 6 (black line)

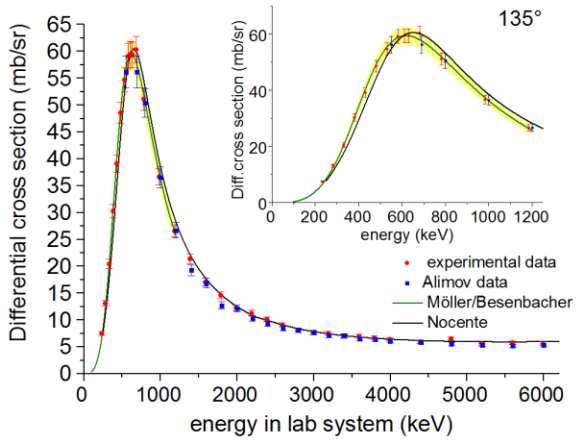

Fig.4 Comparison of differential cross section for 135°

Red points measured data points

Blue points: measured data points from [1]

Green line: differential cross section derived from Möller/Besenbacher

Yellow: uncertainty of Möller/Besenbacher

Black line: calculated differential cross section from Nocente

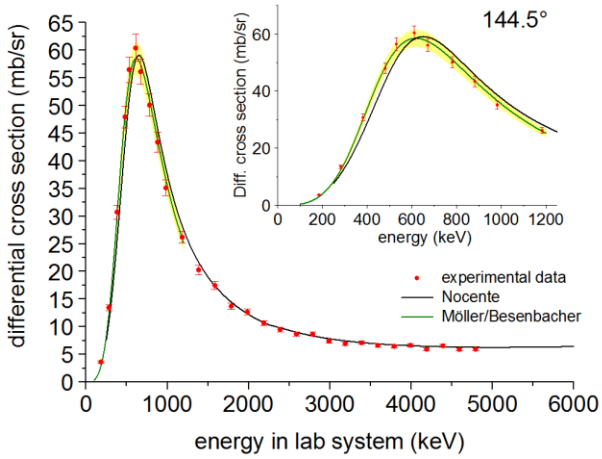

Fig.5 Comparison of differential cross section for 144.5°

Red points measured data points

Green line: differential cross section derived from Möller/Besenbacher

Yellow: error of Möller/Besenbacher

Black line: calculated differential cross section from Nocente

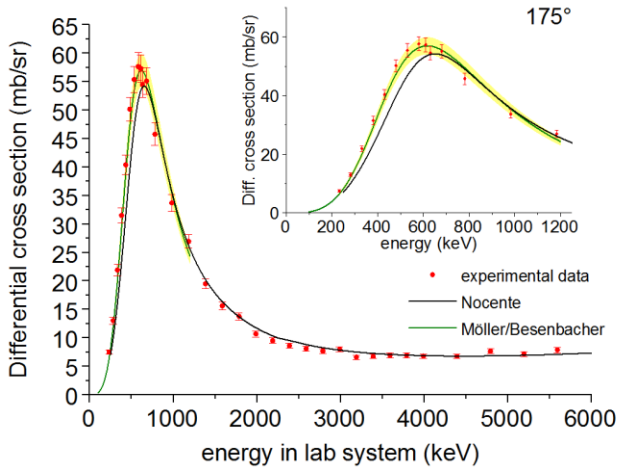

Fig.6 Comparison of differential cross section for 175°

Red points measured data points

Green line: differential cross section derived from Möller/Besenbacher

Yellow: error of Möller/Besenbacher

Black line: calculated differential cross section from Nocente

One can see that Nocente's theoretical curve fits the experimental data for higher energies well. A good description with Nocente's differential cross section is achieved from 1400 keV at 135° and 144.5° or even from 1200 keV at 175°. For lower energies we clearly see differences between the differential cross section from Nocente and the experimental data points. The maxima of both cross sections are not at the same energy, and for lower energies the data points deviate from the theoretical curve. Nocente's cross section is shifted significantly to higher energies at all angles. This shift is not so clearly visible at 135°, but increases at 144.5° and is significant at 175°. For 175° it is even up to 80 keV.

If we fit our experimental data to Nocente's differential cross section for energies between 450 and 600 keV the data won't fit at other energies with a deviation up to 30 %. The question arises whether the parametrization from Bosch and Hale, which was used by Nocente et al. is incorrect for low energies, or if Nocente's et al. conversion to differential cross section is faulty. To answer this question the total cross section from Bosch/Hale is compared to the total cross

section from Möller/Besenbacher in Fig. 7.

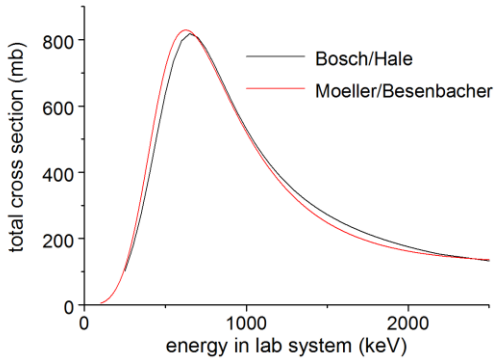

Fig. 7: comparison of the total cross section of Bosch/Hale with the total cross section of Möller/Besenbacher.

It can be recognized that the two cross sections are shifted versus each other at energies below 1200 keV and that the maxima occur at slightly different energies and have different values. This means that the differences in the differential cross sections originate from the parametrization from Bosch/Hale which does not represent the experimental values adequately at low energies. The Bosch and Hale parametrization is based on R-matrix calculations which are based on experimental data before Möller/Besenbacher data were measured. We see that Möller/Besenbacher describe the experimental data more adequately for low energies compared to the parametrization of Bosch and Hale.

A combination of Möller/Besenbacher at energies below 900 keV with Nocente at higher energies provides a good fit to our experimental results.

Summary

In this work the differential cross section for D(^{3}He,p)^{4}He was experimentally determined in the energy range from 0.25 MeV to 5.6 MeV for laboratory angles of 135°, 144.5° and 175°. The data for the reaction angle 135° were compared to already published data and agree within the experimental uncertainties.
All data were compared to the theoretical prediction for the differential cross section from Nocente et al. [7]. For energies below 1 MeV the theoretical values deviate significantly from the

experimental values. At higher energies the theoretical predictions agree well with the experimental data. It was shown that the deviations are due to the parametrization from Bosch/Hale of the total cross section at low energies, which is used by Nocente to calculate the differential cross sections. A combination of Möller/Besenbacher at energies below 900 keV with Nocente at higher energies provides a good fit to our experimental results.

Acknowledgements

The technical assistance at the accelerator laboratory by J.Dorner and M.Fußeder is gratefully acknowledged.

References

[1] V.Kh. Alimov, M. Mayer, J. Roth Nucl. Instr. Meth. B234 (2005) 169

[2] M. Mayer, E. Gauthier, K. Sugiyama, U. von Toussaint, Nucl. Instr. Meth. B267 (2009) 506-512

[3] R.A. Langley S.T. Picraux, F.L. Vook, Journal of Nuclear Materials 53 (1974) 257

[4] K. Schmid, U. von Toissant, Nucl. Instr. Meth. B 281 (2012) 64-71

[5] W. Möller and F. Besenbacher, Nucl. Instr. Meth. 168 (1980) 111

[6] H. S. Bosch and G.M. Hale, Nuclear Fusion, Vol.32(4) (1992) 611

[7] M. Nocente, G.Gorini, J. Källne, M. Tardocchi, Nuclear Fusion 50 (2010) 055001

[8] T. Schwarz-Selinger, A. von Keudell, W. Jacob, Journal of Applied Physics 86, 3988 (1999)

[9] J. Tesmer, M. Nastasi: Handbook of Modern Ion Beam Materials Analysis 1995 Materials Society Pittsburgh USA

[10] T.W. Bonner, J.P. Conner, A.B. Lillie, Phys. Rev. 88 (1952) 473–476.

[11] U. von Toussaint, T. Schwarz-Selinger, M. Mayer, S. Gori, Nuclear Instruments and Methods in Physics Research B 268 (2010) 2115–2118